Nanoscale Research Letters
a SpringerOpen Journal

NANO EXPRESS Open Access

Van der Waals epitaxy and characterization of hexagonal boron nitride nanosheets on graphene

Yangxi Song[1], Changrui Zhang[1*], Bin Li[1], Guqiao Ding[2], Da Jiang[2], Haomin Wang[2] and Xiaoming Xie[2*]

Abstract

Graphene is highly sensitive to environmental influences, and thus, it is worthwhile to deposit protective layers on graphene without impairing its excellent properties. Hexagonal boron nitride (h-BN), a well-known dielectric material, may afford the necessary protection. In this research, we demonstrated the van der Waals epitaxy of h-BN nanosheets on mechanically exfoliated graphene by chemical vapor deposition, using borazine as the precursor to h-BN. The h-BN nanosheets had a triangular morphology on a narrow graphene belt but a polygonal morphology on a larger graphene film. The h-BN nanosheets on graphene were highly crystalline, except for various in-plane lattice orientations. Interestingly, the h-BN nanosheets preferred to grow on graphene than on SiO_2/Si under the chosen experimental conditions, and this selective growth spoke of potential promise for application to the preparation of graphene/h-BN superlattice structures fabricated on SiO_2/Si.

Keywords: Hexagonal boron nitride; Nanosheets; Graphene; van der Waals epitaxy; Chemical vapor deposition

Background

Graphene has attracted global research interests across a wide range of applications [1,2]. However, graphene is highly sensitive to extraneous environmental influences. Thus, it was deemed worthwhile to deposit protective layers over graphene without impairing its properties. Hexagonal boron nitride (h-BN), a well-known dielectric material, may afford the necessary protection for graphene [3,4].

As an analogue of graphene, h-BN shows a minimal lattice mismatch with graphene of about 1.7%, yet has a wide band gap [5-8] and lower environmental sensitivity [3,4]. Hence, h-BN proves to be a promising dielectric material, or substrate, for two-dimensional electronic devices and especially for those based upon the use of graphene [9-13]. Graphene, partially covered by h-BN protective layers, may display promising electronic characteristics of graphene with much lower environmental sensitivity.

Recently, chemical vapor deposition (CVD) synthesis of h-BN on Ni [14-16] or Cu [13,17-19] substrates has been further investigated. For the following applications in graphene electronic devices, h-BN can be acquired by etching of the catalyst substrates and a transfer technique. Nevertheless, the transfer process brings inevitable contamination or even destruction, and it is difficult to determine the position and the coverage ratio of h-BN on graphene. Considering this problem, we pay attention to the catalyst-free CVD growth of h-BN on graphene, which promises direct application in graphene electronic devices and may obviate the need for a transfer process.

It has been demonstrated that van der Waals epitaxy by catalyst-free CVD can be a promising route for the growth of topological heterostructures [20-22]. Moreover, the surface of graphene is atomically flat and without dangling bonds, which makes graphene a promising template for the van der Waals epitaxy of other two-dimensional materials. Compounds with 1:1 B/N stoichiometry are often selected as h-BN precursors for CVD, and borazine ($B_3N_3H_6$) could be a promising choice as it would produce BN and hydrogen, which are both environmentally friendly.

In this research, the van der Waals epitaxy of h-BN nanosheets on mechanically exfoliated graphene by catalyst-free low-pressure CVD, using borazine as the precursor to h-BN, was demonstrated. The h-BN nanosheets preferred to grow on graphene rather than on SiO_2/Si and tended to exhibit a triangular morphology when grown on a narrow

* Correspondence: crzhang12@gmail.com; xmxie@mail.sim.ac.cn
[1]State Key Laboratory of Advanced Ceramic Fibers and Composites, College of Aerospace Science and Engineering, National University of Defense Technology, 109 Deya Road, Changsha 410073, People's Republic of China
[2]State Key Laboratory of Functional Materials for Informatics, Shanghai Institute of Microsystem and Information Technology, Chinese Academy of Sciences, 865 Changning Road, Shanghai 200050, People's Republic of China

graphene belt. The h-BN nanosheets grown on graphene were highly crystalline, albeit with various in-plane lattice orientations.

Methods

h-BN nanosheets were synthesized in a fused quartz tube with a diameter of 50 mm. Graphene was transferred onto silicon oxide/silicon (SiO_2/Si) wafers by mechanical exfoliation from highly oriented pyrolytic graphite (HOPG, Alfa Asear, Ward Hill, MA, USA). The h-BN precursor (borazine) was synthesized by the reaction between $NaBH_4$ and $(NH_4)_2SO_4$ and purified according to our previous reports [23,24]. The temperature for the CVD growth of h-BN nanosheets was set to 900°C. Before the growth of h-BN, with the tube heated to 900°C, graphene grown on SiO_2/Si was first annealed for 60 min in an argon/hydrogen flow (Ar/H_2, 5:1 by volume, both gases were of 99.999% purity from Pujiang Co., Ltd, Shanghai, China) of 180 sccm to remove pollutants remaining on the graphene after mechanical exfoliation. During the growth process, borazine, in a homemade bubbler, was introduced to the growth chamber by another Ar flow of 2 sccm, while the Ar/H_2 flow remained unchanged. The typical growth time was 5 min, while the pressure was 10 to 100 Pa. After the growth process, the tube was rapidly cooled to room temperature.

Raman spectroscopy was performed in a Thermo DXR with 532-nm laser excitation (Thermo Fisher Scientific, Waltham, MA, USA). Atomic force microscopy (AFM) (Dimension Icon, Bruker, Karlsruhe, Germany) and scanning electron microscopy (SEM) (Nova NanoSEM 320, FEI Co., Hillsboro, OR, USA) were used to observe the thickness and morphology of the h-BN nanosheets. X-ray photoelectron spectroscopy (XPS) (AXIS Ultra, Kratos Analytical, Ltd, Manchester, UK) was conducted to analyze the chemical composition of the films. The h-BN nanosheets with the graphene substrate were transferred to transmission electron microscopy (TEM) grids for further characterization. Both morphology images and selected area electron diffraction (SAED) patterns of the h-BN nanosheets were obtained by field emission high-resolution transmission electron microscopy (HRTEM) (Tecnai G^2 20, FEI Co.).

Results and discussion

AFM images (Figure 1) show the morphology and thickness of the h-BN nanosheets. Figure 1a shows the boundary region of SiO_2/Si and graphene with its associated h-BN nanosheets. Figure 1b displays the polygonal morphology of the h-BN nanosheets. It was interesting to note that h-BN nanosheets preferred to grow on graphene rather than on SiO_2/Si.

This result possibly originated from the minimal lattice mismatch between h-BN and graphene, and the small amount of defects remaining in the graphene after mechanical exfoliation and high temperature annealing, and these would enable the h-BN to nucleate on graphene and grow thereafter. This selective growth phenomenon promises potential applications for graphene/h-BN superlattice structures fabricated on SiO_2/Si.

This same phenomenon was also seen in SEM images as shown in Figure 2. Figure 2a shows graphene on SiO_2/Si before CVD, while Figure 2b,c shows h-BN/graphene on SiO_2/Si after CVD. It took time to distinguish graphene from SiO_2/Si due to their low contrast under the SEM as shown in Figure 2a,b where the boundaries of graphene zones on the SiO_2/Si substrate are indicated by arrows. The wrinkles in the graphene in Figure 2a,c originated from the mechanical exfoliation process and could also act as markers indicating the presence of graphene.

The h-BN nanosheets exhibited a polygonal morphology with some nanosheets becoming isolated islands on the graphene, while others with different thicknesses joined and became stacked, as shown in Figure 2c. Moreover, the h-BN nanosheets tended to exhibit a triangular morphology on the much narrower graphene belt, as shown in Figure 2b. This result is similar to van der Waals epitaxial growth of MoS_2 on graphene [21] and perhaps originates from the higher boundary effect of the narrower graphene

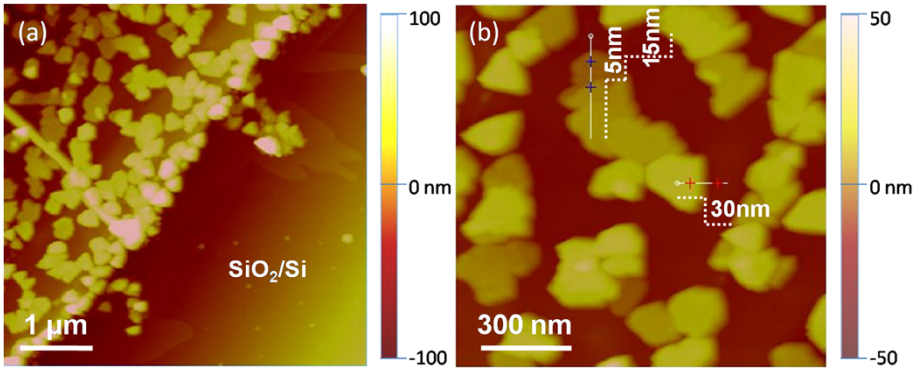

Figure 1 AFM images of h-BN/graphene on SiO_2/Si. (a) Boundary region of h-BN/graphene and SiO_2/Si. **(b)** h-BN nanosheets on graphene.

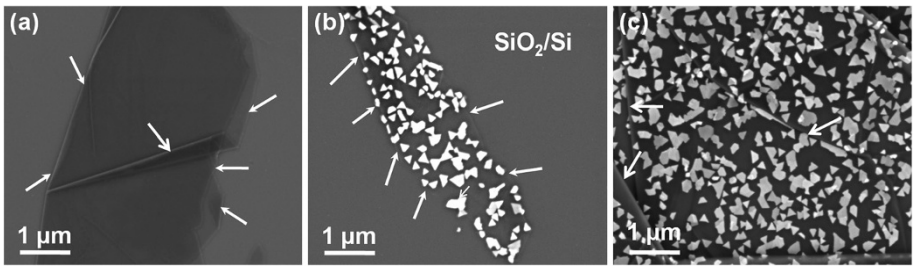

Figure 2 SEM images of graphene and h-BN/graphene on SiO_2/Si. (a) Multilayer graphene on SiO_2/Si before CVD, with the graphene boundary, and wrinkling, indicated by arrows. **(b)** h-BN nanosheets on a narrow graphene belt on SiO_2/Si, with the graphene boundary indicated by arrows. **(c)** h-BN nanosheets on a larger graphene film, with wrinkles indicated by arrows.

belt after mechanical exfoliation [25]. Besides, the triangular h-BN nanosheets on graphene showed different in-plane orientations from each other.

Raman spectroscopy provided a useful means of gleaning information about the lattice vibration modes of graphene and h-BN. After being transferred to SiO_2/Si by the Scotch tape mechanical exfoliation method, the graphene was generally aligned with the (002) lattice plane parallel to the surface of the SiO_2/Si wafer [1,2].

The existence of graphene was shown by Raman spectra in Figure 3, in which the I_{2D}/I_G ratio of graphene was less than 0.5, indicating the multilayer structure of the graphene. Moreover, a weak D peak of graphene at 1,350 cm^{-1} was observed from the Raman spectra (Figure 3), indicating a small number of defects in the graphene, which may have originated from the original HOPG or the mechanical exfoliation process. For the sample examined after CVD, a peak much stronger than the D peak of graphene appeared at 1,367 cm^{-1}, indicating the E_{2g} vibration mode of h-BN, which was consistent with the reported values [5,6,13-19]. Interestingly, the 2D and G peaks for graphene diminished in intensity after CVD, and this may have originated from the partial coverage of the graphene by h-BN. As shown in Figure 3b,c, the G peaks of graphene for the graphene substrate and h-BN/graphene were fitted with Lorentz curves (solid lines). The fitting data were well fitted with the raw data, while the Raman frequency and full width at half maximum (FWHMs) for G bands were almost equal to each other. These results are comparable with the reported values of graphene [26] and graphite [27,28], showing the high quality of graphene before and after CVD and indicating that the synthesis of h-BN nanosheets on graphene in our manuscript does not cause a degradation of graphene.

According to previous reports [29], the gas-phase nucleation for h-BN was absent at growth temperatures lower than 1,000°C; hence, the growth of h-BN nanosheets on graphene was dominated by the surface nucleation during our CVD process at 900°C. Moreover, the surface topography of the substrate is vital to the surface nucleation [30]. Consequently, the nucleation of the h-BN nanosheets on the graphene substrate was regulated by the surface morphology of graphene in our work. Additionally, the atomic scale defects, dislocations, and

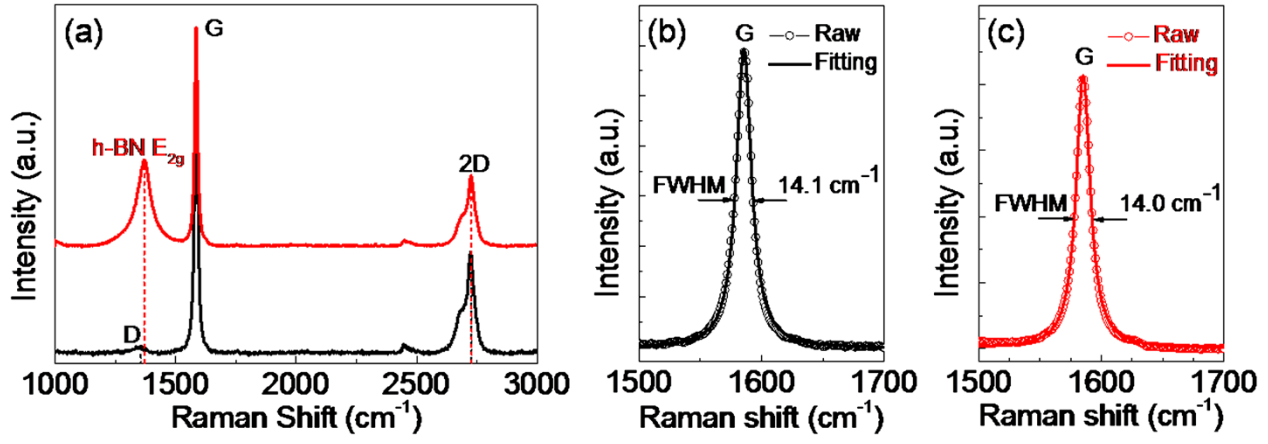

Figure 3 Raman spectra. (a) Raman spectra of graphene before CVD (lower plot) and h-BN/graphene after CVD (upper plot). G peaks fitting with Lorentz curves (solid lines) for graphene substrate **(b)** and h-BN/graphene **(c)** are shown with their FWHMs, respectively.

steps for the graphene substrate were inevitable during the mechanical exfoliation process due to the strong interlayer binding of graphite [31], and the atomic-level defects, dislocations, and steps of the substrates would serve as the nucleation centers for CVD growth, for the curved sp2 π bonds in the graphene defects, dislocations, and steps were more reactive than the planar graphene regions [21,32]. In our work, a small number of defects for the graphene substrates were proved by the weak D peak of Raman spectra in Figure 3. The atomic defects offer additional bond sites to the carbon atoms, making them energetically preferred for nucleation. During the CVD growth, the atomic-level defects of graphene could effectively cause nucleation of the h-BN on the graphene. Subsequently, with an increased amount of precursor, the h-BN nanosheets could grow on the surface of graphene through weak van der Waals interactions.

XPS was used to analyze the chemical composition of the h-BN/graphene on the surface of the SiO_2/Si, as shown in Figure 4. The raw XPS data were corrected using the binding energy of the C-C bond at 284.5 eV. The Si and O peaks in Figure 4 arose from the SiO_2/Si substrate, while the C peak arose from the presence of graphene. The binding energies of B1s and N1s from the XPS spectra were 191.0 and 398.5 eV, respectively, which were in good agreement with reported values [14,16,18,19,33,34] for h-BN. The B/N ratio of the sample, as taken from the XPS measurement, was 1.01, indicating the nearly stoichiometric composition of the synthesized h-BN nanosheets on graphene. As shown in Figure 4b,c,d, the XPS peaks of B1s, N1s, and C1s core levels were fitted with Gaussian curves (red peaks). The fitting data were well fitted with the raw data, and no shoulder peaks could be observed from the fitting curves. Hence, the single peaks of fitting data indicate that the C-B or C-N bonds do not exist in our h-BN/graphene system, compared with the reported results of BCN films [35,36]. These results show that the synthesis of h-BN nanosheets on graphene in our manuscript does not cause a degradation of graphene.

We have pointed out the reason for the nucleation of the h-BN on graphene. In fact, the deposition of h-BN nanosheets on graphene was performed as instantaneous nucleation followed by three-dimensional growth in our catalyst-free CVD growth. Similar results of three-dimensional growth in certain situations have been proved by previous reports [21,32]. As discussed above, energy optimization is of great importance to the nucleation of h-BN, and the defects, dislocations, and steps of graphene are energetically preferred. During the CVD growth of h-BN on graphene, the above energetically preferred regions of graphene would be covered or remedied by h-BN layers with a certain domain size. As an alternative, the edges of the as-grown h-BN layers and the regions near the defects of graphene turned energetically preferred for nucleation of new h-BN layers, which both favor the vertical or three-dimensional growth of h-BN nanosheets on the graphene.

After the h-BN nanosheets on graphene were transferred to TEM grids after the etching of SiO_2/Si, atomic resolution HRTEM was used to study the crystalline structure of the aforementioned h-BN nanosheets on

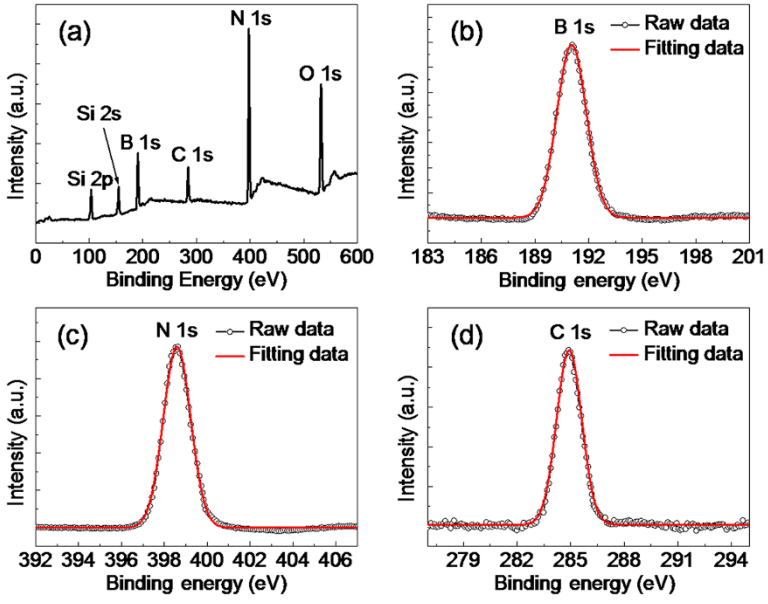

Figure 4 XPS spectra of h-BN/graphene on SiO_2/Si. (a) Survey spectrum. **(b-d)** XPS spectra of B1s, N1s, and C1s core levels, respectively. The peaks of (b-d) were fitted with Gaussian curves (red peaks), and good fits could be observed for the raw data and the fitting data.

their respective graphene substrates. Figure 5a shows a TEM image of the h-BN nanosheets on graphene, with the arrows indicating the edge of the graphene. The polygonal objects on the graphene indicated the existence of h-BN nanosheets. The numbers '1' to '4' indicate typical regions of Figure 5a. Region 1 refers to a region of graphene without any h-BN nanosheet thereon, while regions 2 to 4 refer to isolated h-BN nanosheets on the graphene. Figure 5b,c,d shows the atomic images corresponding to regions 2 to 4, while the corresponding SAED patterns for regions 1 to 4 are shown in Figure 5e, f,g,h, respectively. The regular, periodic SAED spots evinced the high degree of crystallinity of both the graphene and h-BN nanosheets.

Figure 5b shows that the h-BN nanosheet in region 2 had the same in-plane lattice orientation as the graphene substrate. However, the h-BN nanosheets and graphene in regions 3 and 4 were rotationally displaced, according to their Moiré patterns (see insets of Figure 5c,d, respectively). The h-BN nanosheets on graphene had various in-plane lattice orientations, which were consistent with the SAED patterns of Figure 5f,h. These results were also evinced by the SEM image (Figure 2b), as the triangular h-BN nanosheets on the narrow graphene belt also lay in various directions.

Conclusions

In summary, we have demonstrated the van der Waals epitaxy of h-BN nanosheets on graphene by catalyst-free CVD, which may maintain the promising electronic characteristics of graphene. The h-BN nanosheets tended to have a triangular morphology on a narrow graphene belt, whereas they had a polygonal morphology on a much larger graphene film. The B/N ratio of the h-BN nanosheets

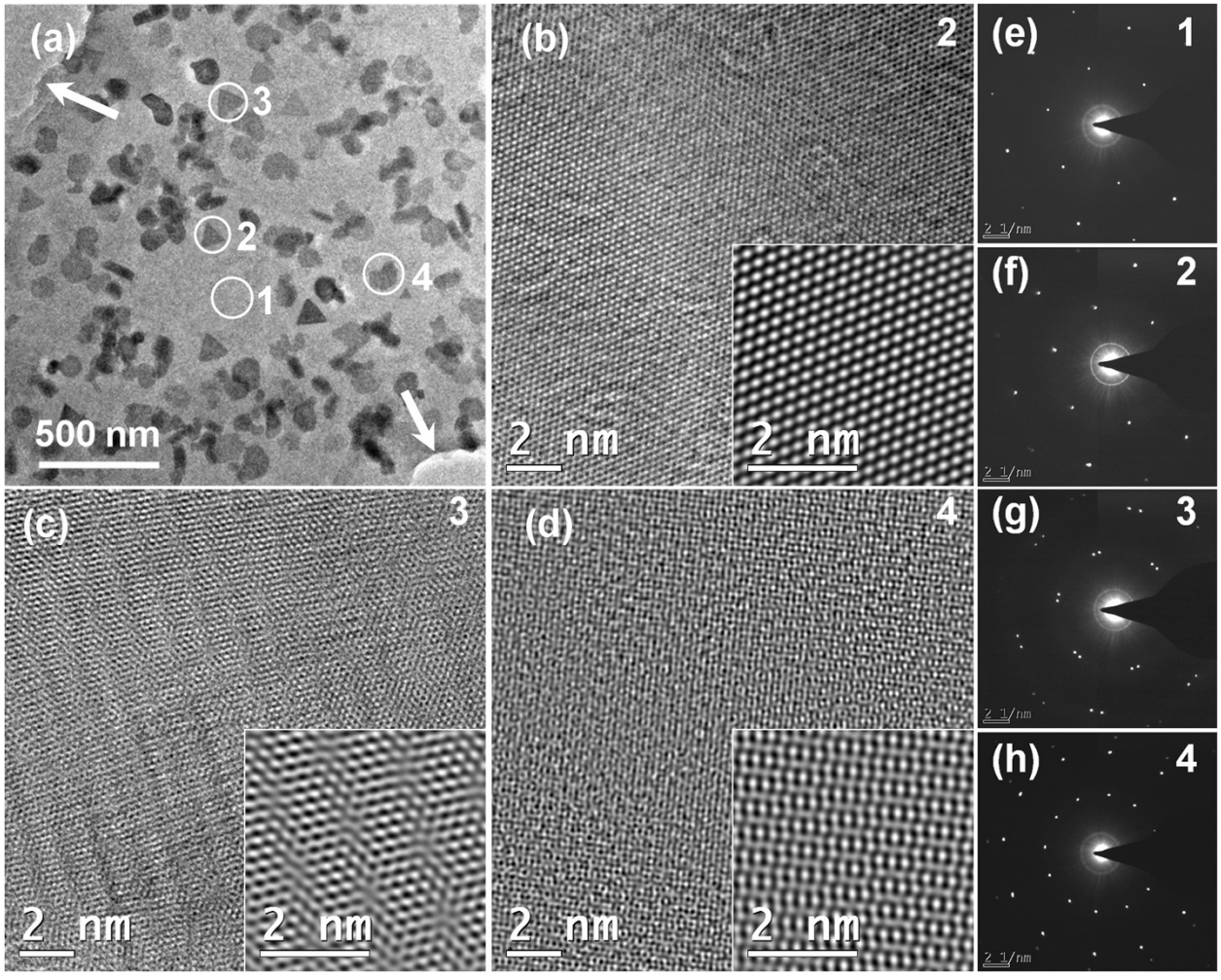

Figure 5 Images of h-BN/graphene transferred onto TEM grids. (a) A low-magnification TEM image of h-BN nanosheets on graphene, with the arrows showing the graphene boundary. **(b-d)** HRTEM atomic images corresponding to regions 2, 3, and 4 in (a), with the insets showing FFT-filtered images, respectively. **(e-h)** SAED patterns corresponding to regions 1 to 4.

on graphene was 1.01, indicative of an almost stoichiometric composition of h-BN. The h-BN nanosheets preferred to grow on graphene rather than on SiO_2/Si, which offered the promise of potential applications for the preparation of graphene/h-BN superlattice structures. The h-BN nanosheets on graphene had a high degree of crystallinity, except for various in-plane lattice orientations. The synthesis of h-BN nanosheets on multilayer graphene has been studied, and h-BN nanosheets on few-layer and even monolayer graphene will be synthesized in future work. This may satisfy certain application requirements for topological heterostructures and graphene-related electronic devices.

Competing interests

The authors declare that they have no competing interests.

Authors' contributions

YS, CZ, BL, and XX designed the experiments, and YS carried out most of the experimental work and material characterizations. CZ and BL synthesized the borazine. YS, CZ, BL, GD, and XX discussed the results, and YS drafted the manuscript. All authors have read and approved the final manuscript.

Acknowledgements

This work was financially supported by projects from the Natural Science Foundation of China (Grant Nos. 11104303, 11274333, 11204339, 61136005, and 50902150), Chinese Academy of Sciences (Grant Nos. KGZD-EW-303, XDA02040000, and XDB04010500), the Open Foundation of State Key Laboratory of Functional Materials for Informatics (Grant No. SKL201309), the National High-tech R & D Programme (Grant No. 2012AA7024034), and the National Science and Technology Major Projects of China (Grant No. 2011ZX02707). We thank the anonymous reviewers for their helpful suggestions which have improved the manuscript.

Received: 9 May 2014 Accepted: 21 July 2014
Published: 28 July 2014

References

1. Novoselov KS, Geim AK, Morozov SV, Jiang D, Zhang Y, Dubonos SV, Grigorieva IV, Firsov AA: **Electric field effect in atomically thin carbon films.** *Science* 2004, **306:**666–669.
2. Novoselov KS, Jiang D, Schedin F, Booth TJ, Khotkevich VV, Morozov SV, Geim AK: **Two-dimensional atomic crystals.** *Proc Natl Acad Sci U S A* 2005, **102:**10451–10453.
3. Wang L, Chen Z, Dean CR, Taniguchi T, Watanabe K, Brus LE, Hone J: **Negligible environmental sensitivity of graphene in a hexagonal boron nitride/graphene/h-BN sandwich structure.** *ACS Nano* 2012, **6:**9314–9319.
4. Han Q, Yan B, Gao T, Meng J, Zhang Y, Liu Z, Wu X, Yu D: **Boron nitride film as a buffer layer in deposition of dielectrics on graphene.** *Small* 2014, **10:**2293–2299.
5. Watanabe K, Taniguchi T, Kanda H: **Direct-bandgap properties and evidence for ultraviolet lasing of hexagonal boron nitride single crystal.** *Nat Mater* 2004, **3:**404–409.
6. Kubota Y, Watanabe K, Tsuda O, Taniguchi T: **Deep ultraviolet light-emitting hexagonal boron nitride synthesized at atmospheric pressure.** *Science* 2007, **317:**932–934.
7. Guo N, Wei J, Jia Y, Sun H, Wang Y, Zhao K, Shi X, Zhang L, Li X, Cao A, Hongwei Z, Kunlin W, Dehai W: **Fabrication of large area hexagonal boron nitride thin films for bendable capacitors.** *Nano Res* 2013, **6:**602–610.
8. Meng X-L, Lun N, Qi Y-X, Zhu H-L, Han F-D, Yin L-W, Fan R-H, Bai Y-J, Bi J-Q: **Simple synthesis of mesoporous boron nitride with strong cathodoluminescence emission.** *J Solid State Chem* 2011, **184:**859–862.
9. Kim KK, Hsu A, Jia X, Kim SM, Shi Y, Dresselhaus M, Palacios T, Kong J: **Synthesis and characterization of hexagonal boron nitride film as a dielectric layer for graphene devices.** *ACS Nano* 2012, **6:**8583–8590.
10. Sachdev H, Müller F, Hüfner S: **BN analogues of graphene: on the formation mechanism of boronitrene layers - solids with extreme structural anisotropy.** *Diam Relat Mater* 2010, **19:**1027–1033.
11. Gannett W, Regan W, Watanabe K, Taniguchi T, Crommie MF, Zettl A: **Boron nitride substrates for high mobility chemical vapor deposited graphene.** *Appl Phys Lett* 2011, **98:**242105.
12. Dean CR, Young AF, Meric I, Lee C, Wang L, Sorgenfrei S, Watanabe K, Taniguchi T, Kim P, Shepard KL, Hone J: **Boron nitride substrates for high-quality graphene electronics.** *Nat Nanotechnol* 2010, **5:**722–726.
13. Lee KH, Shin HJ, Lee J, Lee IY, Kim GH, Choi JY, Kim SW: **Large-scale synthesis of high-quality hexagonal boron nitride nanosheets for large-area graphene electronics.** *Nano Lett* 2012, **12:**714–718.
14. Shi Y, Hamsen C, Jia X, Kim KK, Reina A, Hofmann M, Hsu AL, Zhang K, Li H, Juang ZY, Dresselhaus MS, Li L-J, Kong J: **Synthesis of few-layer hexagonal boron nitride thin film by chemical vapor deposition.** *Nano Lett* 2010, **10:**4134–4139.
15. Auwärter W, Suter HU, Sachdev H, Greber T: **Synthesis of one monolayer of hexagonal boron nitride on Ni(111) from B-trichloroborazine $(ClBNH)_3$.** *Chem Mater* 2004, **16:**343–345.
16. Lee Y-H, Liu K-K, Lu A-Y, Wu C-Y, Lin C-T, Zhang W, Su C-Y, Hsu C-L, Lin T-W, Wei K-H, Shi Y, Li L-J: **Growth selectivity of hexagonal-boron nitride layers on Ni with various crystal orientations.** *RSC Adv* 2012, **2:**111–115.
17. Kim KK, Hsu A, Jia X, Kim SM, Shi Y, Hofmann M, Nezich D, Rodriguez-Nieva JF, Dresselhaus M, Palacios T, Kong J: **Synthesis of monolayer hexagonal boron nitride on Cu foil using chemical vapor deposition.** *Nano Lett* 2012, **12:**161–166.
18. Song L, Ci L, Lu H, Sorokin PB, Jin C, Ni J, Kvashnin AG, Kvashnin DG, Lou J, Yakobson BI, Ajayan PM: **Large scale growth and characterization of atomic hexagonal boron nitride layers.** *Nano Lett* 2010, **10:**3209–3215.
19. Guo N, Wei J, Fan L, Jia Y, Liang D, Zhu H, Wang K, Wu D: **Controllable growth of triangular hexagonal boron nitride domains on copper foils by an improved low-pressure chemical vapor deposition method.** *Nanotechnology* 2012, **23:**415605.
20. Yan K, Peng H, Zhou Y, Li H, Liu Z: **Formation of bilayer Bernal graphene: layer-by-layer epitaxy via chemical vapor deposition.** *Nano Lett* 2011, **11:**1106–1110.
21. Shi Y, Zhou W, Lu AY, Fang W, Lee YH, Hsu AL, Kim SM, Kim KK, Yang HY, Li LJ, Idrobo JC, Kong J: **Van der Waals epitaxy of MoS_2 layers using graphene as growth templates.** *Nano Lett* 2012, **12:**2784–2791.
22. Hwang J, Kim M, Campbell D, Alsalman HA, Kwak JY, Shivaraman S, Woll AR, Singh AK, Hennig RG, Gorantla S: **Van der Waals epitaxial growth of graphene on sapphire by chemical vapor deposition without a metal catalyst.** *ACS Nano* 2012, **7:**385–395.
23. J-s L, C-r Z, Li B, Cao F, Wang SQ: **An investigation on the synthesis of borazine.** *Inorg Chim Acta* 2011, **366:**173–176.
24. J-s L, C-r Z, Li B, Cao F, Wang SQ: **An improved synthesis of borazine with aluminum chloride as catalyst.** *Eur J Inorg Chem* 2010, **2010:**1763–1766.
25. Lima MP, Fazzio A, da Silva AJR: **Edge effects in bilayer graphene nanoribbons: ab initio total-energy density functional theory calculations.** *Phys Rev B* 2009, **79:**153401.
26. Calizo I, Balandin A, Bao W, Miao F, Lau C: **Temperature dependence of the Raman spectra of graphene and graphene multilayers.** *Nano Lett* 2007, **7:**2645–2649.
27. Tan PH, Dimovski S, Gogotsi Y: **Raman scattering of non-planar graphite: arched edges, polyhedral crystals, whiskers and cones.** *Phil Trans R Soc Lond A* 2004, **362:**2289–2310.
28. Tan PH, Deng YM, Zhao Q, Cheng WC: **The intrinsic temperature effect of the Raman spectra of graphite.** *Appl Phys Lett* 1999, **74:**1818.
29. Li JS, Zhang CR, Li B: **Preparation and characterization of boron nitride coatings on carbon fibers from borazine by chemical vapor deposition.** *Appl Surf Sci* 2011, **257:**7752–7757.
30. Zhang XW, Boyen HG, Deyneka N, Ziemann P, Banhart F, Schreck M: **Epitaxy of cubic boron nitride on (001)-oriented diamond.** *Nat Mater* 2003, **2:**312–315.
31. Allen MJ, Tung VC, Kaner RB: **Honeycomb carbon: a review of graphene.** *Chem Rev* 2009, **110:**132–145.
32. Tang S, Ding G, Xie X, Chen J, Wang C, Ding X, Huang F, Lu W, Jiang M: **Nucleation and growth of single crystal graphene on hexagonal boron nitride.** *Carbon* 2012, **50:**329–331.
33. Nagashima A, Tejima N, Gamou Y, Kawai T, Oshima C: **Electronic dispersion relations of monolayer hexagonal boron nitride formed on the Ni(111) surface.** *Phys Rev B* 1995, **51:**4606–4613.

34. Wang W-L, Bi J-Q, Sun W-X, Zhu H-L, Xu J-J, Zhao M-T, Bai Y-J: **Facile synthesis of boron nitride coating on carbon nanotubes.** *Mater Chem Phys* 2010, **122:**129–132.
35. Ci L, Song L, Jin C, Jariwala D, Wu D, Li Y, Srivastava A, Wang ZF, Storr K, Balicas L, Liu F, Ajayan PM: **Atomic layers of hybridized boron nitride and graphene domains.** *Nat Mater* 2010, **9:**430–435.
36. Yue J, Cheng W, Zhang X, He D, Chen G: **Ternary BCN thin films deposited by reactive sputtering.** *Thin Solid Films* 2000, **375:**247–250.

doi:10.1186/1556-276X-9-367
Cite this article as: Song *et al.*: Van der Waals epitaxy and characterization of hexagonal boron nitride nanosheets on graphene. *Nanoscale Research Letters* 2014 **9**:367.